Tapered Hygo-Thermally Curvature-Stable Laminates with Non-Standard Ply Orientations.

Christopher B. York[a]

[a]University of Glasgow,
School of Engineering,
James Watt (South) Building,
Glasgow G12 8QQ
UK
Christopher.York@Glasgow.ac.uk
T: +44(0) 141 3304345
F: +44(0) 141 3305560

Abstract: Stacking sequence configurations for hygro-thermally curvature-stable (HTCS) laminates have recently been identified in nine unique classes of coupled laminate with standard ply angle orientations +45, −45, 0 and 90°. All arise from the judicious re-alignment of the principal material axis of laminate classes with Bending-Twisting and/or Bending-Extension and Twisting-Shearing coupling; where off-axis material alignment of these parent classes gives rise to distinctly different mechanical coupling behaviour. However, for standard ply angle orientations, HTCS solutions were found in only 8-, 12-, 16- and 20-ply laminates.
This article considers non-standard ply angle orientations +60, −60, 0 and 90°, which lead to solutions in all ply number groupings for 10 plies and above, thus offering a possibility for ply terminations and hence tapered HTCS laminate designs.

Keywords:
A. Laminates; B. Thermomechanical; C. Laminate mechanics

1. Introduction

Tailored composite laminates possessing complex mechanical coupling are beginning to find application beyond the aerospace sector, with which they have been traditionally associated, and towards new and emerging applications, but only where certification is less stringent or design rules have not become entrenched or risk averse. For example, mechanically coupled composite materials offer great potential as an enabling technology in very large offshore wind turbine blades where the mechanical coupling may serve as a passive load-alleviation mechanism during extreme wind conditions, and where failure of an active control system may lead to destruction of the entire wind turbine. Recent research [1,2] has demonstrated that there is a vast and unexplored laminate design space containing exotic forms of mechanical coupling, which includes all interactions between Extension, Shearing, Bending and Twisting, but more importantly, that a broad range of these mechanical coupling responses can be achieved without the undesirable thermal distortions that result from the high temperature curing process. Such laminate designs may be described as hygro-thermally curvature-stable (HTCS)[1].

[1] Hygro-Thermally Curvature-Stable is henceforth abbreviated to HTCS

HTCS laminate designs may help to raise interest in the potential for exploiting mechanically coupled materials, particularly from a manufacturing perspective. However, the requirement for tapering the laminate thickness remains a major design constraint, given that this is achieved by terminating either single or multiple ply layers in the laminate. For mechanically coupled HTCS laminates, tapering represents a significant challenge because, invariably, mechanical behaviour changes substantially and immunity to thermal distortion is destroyed when plies are dropped, or terminated. To put this issue into context, the remainder of this introductory section will present a brief overview of the state of the art in coupled HTCS laminates. The complete range of mechanically coupled behaviour, achievable with HTCS laminates, will then be described in the section following. Thereafter, details of: the development of HTCS laminates with non-standard ply orientations; the number of solutions and abridged stacking sequence listings and; the magnitude of mechanical coupling, compared with standard ply orientation designs, will be given. Finally, the scope for tapered laminate designs will be discussed and new tapered laminate configurations presented, for which mechanical coupling and immunity to thermal distortion are maintained.

1.1 State of the art in coupled HTCS laminates

The design of aero-elastic compliant rotor blades with tailored Extension-Twisting coupling is a design concept that requires either specially curved tooling or HTCS properties in order to maintain the desired shape after high temperature curing. Winckler [3] is credited with being the first to discover a solution: an eight-ply HTSC configuration, developed by using the concept of bonding two (or more) symmetric cross-ply $[○/●/●/○]_T$ sub-laminates, where each sub-laminate is counter-rotated by $\pi/8$, giving rise to the laminate: $[22.5/-67.5_2/22.5/-22.5/67.5_2/-22.5]_T$, which possesses Extension-Twisting and Shearing-Bending coupling. Winckler [3] recognized that the symmetric cross-ply sub-laminate represents a HTCS configuration, which remains so after rotation and/or combining with additional sub-laminates through either stacking or interlacing.

Chen [4] used an optimisation procedure to maximise the Extension-Twisting coupling of the laminate and investigated several different sub-sequence forms to achieve this. All coupled laminate results were based on 16-ply configurations, optimised for maximum mechanical coupling compliance (b_{16}). The first configuration, based on the most general form: $[\theta_1/\theta_2/...../\theta_{16}]_T$ gave the following optimum sequence: $[14.62/16.21/-69.56/21.63/-66.34/-59.38/-55.98/-49.52/49.13/56.01/61.46/64.36/-21.3/69.04/-17.01/-14.88]_T$.

Cross et al. [5] augmented the theoretical proofs of Chen [4] for the necessary conditions for HTCS coupled laminates, focussing also on maximising the mechanical coupling response, but now with the smallest possible ply number groupings. A 5-ply anti-symmetric configuration was derived: $[76.3/-33.6/0/33.6/-76.3]_T$. The article also included numerical and experimental validation to assess the robustness of the designs due to ply orientation errors. However, conclusions were drawn entirely on the basis of the anti-symmetric 6-ply solution: $[15/-75/-45]_A$.

A number of subsequent articles have substantially extended this work; the focus, however, remaining almost entirely on maximising the mechanical compliance (b_{16}) using free form orientations rather than standard ply orientations. Only the most recent

work [6] has considered combined mechanical coupling, i.e., Extension-Twisting and Bending-Twisting coupling behaviour at the laminate level.
Weaver [7] derived the conditions for HTCS laminates independently. The article presents an elegant and compact form of the lamination parameter equations, which describe the necessary conditions for HTCS laminates, but are otherwise identical to those previously derived by Chen [4]. The laminate configurations presented were restricted entirely to the principal of repeating groups containing four-ply symmetric sub-sequences with orthogonal orientations, and to standard angle-ply configurations, which demonstrate a number of the laminate forms postulated by Winckler [3]. The resulting configurations are repeated here for completeness: $[0/90/90/0/\underline{45/-45/-45/45}]_T$, $[90/0/0/\ 90/60/-30/-30/60]_T$, $[0/\underline{45}/90/\underline{-45}/90/\underline{-45}/0/\underline{45}]_T$, $[0/90/\underline{45/-45}/90/0/\underline{-45/45}]_T$, $[90/\underline{45/-45}/0/\underline{-45/45}/0/\underline{-45/45}/90/\underline{45/-45}]_T$, where the repeating 0/90/90/0 sub-laminate is rotated by 45° in the first solution, and by 90° and 60°, respectively, in the second. The concept of sub-laminate 'splicing', proposed by Tsai [8], was also shown to be applicable to coupled HTCS laminates with repeating sub-laminate groupings, whereby an underscore identifies the plies of one sub-laminate which have been 'spliced' or, more appropriately, 'interlaced' with another sub-laminate.
Stacking sequence configurations for HTCS laminates have recently [2] been identified in 9 unique classes of coupled laminate with standard ply angle orientations +45, −45, 0 and 90°. All arise from the judicious re-alignment of the principal material axis of parent laminate classes with Bending-Twisting and/or Bending-Extension and Twisting-Shearing coupling. Off-axis material alignment of these parent classes gives rise to more complex combinations of mechanical coupling behaviour, but also to isolated coupling responses in some cases. For standard ply angle orientations, HTCS solutions were however found in only 8-, 12-, 16- and 20-ply laminates; the study being limited to a maximum of 21 plies; a range deemed to be representative of thin laminates.

2. Characterization of thermo-mechanical properties.

Laminated composite materials have recently been characterized [1] in terms of their response to mechanical and/or thermal loading, to help understand the new classes of coupled laminate behaviour described in this article. This characterisation process provides a detailed description of coupling behaviour, not present in conventional materials, and which is often misunderstood.
It is well known that coupling exists between in-plane (i.e., extension or membrane) and out-of-plane (i.e., bending or flexure) responses when $B_{ij} \neq 0$ in Eq. (1), and between in-plane shear and extension when $A_{16} = A_{26} \neq 0$, and between out-of-plane bending and twisting when $D_{16} = D_{26} \neq 0$.

$$\begin{Bmatrix} N_x \\ N_y \\ N_{xy} \end{Bmatrix} = \begin{bmatrix} A_{11} & A_{12} & A_{16} \\ & A_{22} & A_{26} \\ \text{Sym.} & & A_{66} \end{bmatrix} \begin{Bmatrix} \varepsilon_x \\ \varepsilon_y \\ \gamma_{xy} \end{Bmatrix} + \begin{bmatrix} B_{11} & B_{12} & B_{16} \\ & B_{22} & B_{26} \\ \text{Sym.} & & B_{66} \end{bmatrix} \begin{Bmatrix} \kappa_x \\ \kappa_y \\ \kappa_{xy} \end{Bmatrix}$$
$$\begin{Bmatrix} M_x \\ M_y \\ M_{xy} \end{Bmatrix} = \begin{bmatrix} B_{11} & B_{12} & B_{16} \\ & B_{22} & B_{26} \\ \text{Sym.} & & B_{66} \end{bmatrix} \begin{Bmatrix} \varepsilon_x \\ \varepsilon_y \\ \gamma_{xy} \end{Bmatrix} + \begin{bmatrix} D_{11} & D_{12} & D_{16} \\ & D_{22} & D_{26} \\ \text{Sym.} & & D_{66} \end{bmatrix} \begin{Bmatrix} \kappa_x \\ \kappa_y \\ \kappa_{xy} \end{Bmatrix} \qquad (1)$$

where the force and moment resultant vector components account for the combined effects of thermal, mechanical and hygral loading.

Whilst Eq. (1) describes the well-known **ABD** relation from classical lamination theory, it is essential to adopt a more compact notation when describing a specific class of coupled laminate. By re-casting Eq. (1) as:

$$\begin{Bmatrix} \mathbf{N} \\ \mathbf{M} \end{Bmatrix} = \begin{bmatrix} \mathbf{A} & \mathbf{B} \\ \mathbf{B} & \mathbf{D} \end{bmatrix} \begin{Bmatrix} \boldsymbol{\varepsilon} \\ \boldsymbol{\kappa} \end{Bmatrix} \qquad (2)$$

the coupling behaviour, which is clearly dependent on the form of the elements in each of the extensional [**A**], coupling [**B**] and bending [**D**] stiffness matrices is now described by an extended subscript notation, defined previously by the Engineering Sciences Data Unit [9]. Hence, balanced and symmetric stacking sequences, which generally possess coupling between bending and twisting, are referred to by the designation $\mathbf{A}_S\mathbf{B}_0\mathbf{D}_F$, signifying that the elements of the extensional stiffness matrix [**A**] are specially orthotropic in nature, i.e., uncoupled, since

$$A_{16} = A_{26} = 0, \qquad (3)$$

the bending-extension coupling matrix [$\mathbf{B}_0$] is null, whilst all elements of the bending stiffness matrix [$\mathbf{D}_F$] are finite, i.e., $D_{ij} \neq 0$.
Laminates possessing coupling between in-plane shear and extension only are, by the same rationale, referred to by the designation $\mathbf{A}_F\mathbf{B}_0\mathbf{D}_S$, signifying that all elements of the extensional stiffness matrix [$\mathbf{A}_F$] are finite, i.e., $A_{ij} \neq 0$, the bending-extension coupling matrix [$\mathbf{B}_0$] is null, and the elements of the bending stiffness matrix [$\mathbf{D}_S$] are specially orthotropic in nature, i.e., uncoupled, since

$$D_{16} = D_{26} = 0 \qquad (4)$$

The extensional [**A**] and bending [**D**] stiffness matrices possess one of two forms: uncoupled [$\mathbf{A}_S/\mathbf{D}_S$] or coupled [$\mathbf{A}_F/\mathbf{D}_F$]. The fully uncoupled form [$\mathbf{A}_S\mathbf{B}_0\mathbf{D}_S$] can be described as a *Simple* laminate, whereas the coupled forms may be described in terms of the response that the laminate exhibits to various combination of force and moment resultants, using a *cause* and *effect* relationship. A laminate is therefore described as an *E-S* laminate if *Extension* (*E*) causes a *Shearing* (*S*) effect, whereas if *Bending* causes a *Twisting* effect then the laminate is described as a *B-T* laminate. Each *cause* and *effect* relationship is reversible.
In contrast to the uncoupled and coupled form of the extensional [**A**] and bending [**D**] stiffness matrices, which are described in Table 1(a) and (c) with respect to the form of the laminate and coupling description, respectively, the coupling [**B**] stiffness matrix has several complex forms: $\mathbf{B}_0$ in the preceding laminate descriptions must now be replaced with alternative designations given in Table 1(b), noting that only those relevant to the current article are given here.
The response-based labelling is developed fully in the captions of Figs 1 - 3, which demonstrate the type of thermal warping behaviour that generally arises due to the high temperature curing process, in which cooling takes place without mechanical or

geometrical constraints; example stacking sequences are representative of the minimum ply number grouping for each laminate class. The HTCS laminate designs presented later in this article have immunity to such thermal warping distortions, whilst maintaining the mechanical coupling responses corresponding to the nine laminate classes presented Figs 1 - 3.
The response-based labelling is complementary to the Engineering Sciences Data Unit subscript notation [9]. Note that each *cause* and *effect* pair is underlined and the semi-colon, e.g., *E-S*;*B-S*-*T-E*;*B-T*, is used to differentiate between couplings due to the extensional [**A**] stiffness matrix, coupling [**B**] stiffness matrix and bending [**D**] stiffness matrix, respectively. The subscripts for the coupling [**B**] matrix, given in Table 1(b), follow exactly the same logic as described for the extensional [**A**] and bending [**D**] matrices in Table 1(a) and (c), respectively. The complexities of the [**B**] matrix relating to this article are in fact captured by only one additional subscript: Subscript *t* denotes that off-diagonal (or *t*ransverse) elements ($B_{16} = B_{26} \neq 0$) are non-zero.

The illustrations in Figs 1 - 3 represent classical laminated plate theory predictions that are well known to be correct only when side length to thickness ratio is small. Recent experimental results [10] have in fact shown this to be the case over a much broader range of coupled laminate classes than previously investigated; however, exceptions were also discovered.

3. Development of hygro-thermally curvature-stable (HTCS) laminates designs.

Definitive listings of coupled laminates have recently [1] been derived for 24 unique classes of coupled laminate from which the nine HTCS sub-classes described above have subsequently been derived. These definitive listings were derived in symbolic form, together with non-dimensional parameters; making each laminate class independent of both fibre orientations and material properties.
The following describes the significance of the non-dimensional parameters and how they may be used to: develop stiffness relations for a given configuration; assess the thermal response of a particular configuration and; demonstrate the necessary conditions for HTCS response.
It is recognized that behaviour due to changes in temperature and moisture content are synonymous in the context of hygro-thermally curvature-stable design, where the associated thermal and moisture expansion coefficients are interchangeable. However, it is recognised that hygral and thermal behaviour are similar only when temperature and moisture content have reached equilibrium and their distributions throughout the laminate are uniform, which is very often not the case, as the characteristic times for equilibrium are significantly different. Therefore, discussion is restricted to the thermal loading condition in the remainder of this article.

3.1 Development of stiffness relations.

The calculation of non-dimensional coupling stiffness parameters is readily demonstrated for the 8-ply laminate $[+/O/-/O/-/\bullet/+/O]_T$, where elements of coupling stiffness matrix,

$$B_{ij} = \Sigma Q'_{ij,k} (z_k^2 - z_{k-1}^2)/2 \qquad (5)$$

where the summation may instead be written in sequence order for the eight individual plies, and where *z*, representing the distance from the laminate mid-plane, is expressed here in terms of the uniform ply thickness *t*:

$$B_{ij} = \{Q'_{ij+}((-3t)^2 - (-4t)^2) + Q'_{ij_\circ}((-2t)^2 - (-3t)^2) + Q'_{ij-}((-t)^2 - (-2t)^2) + Q'_{ij_\circ}((0)^2 - (-t)^2) + Q'_{ij-}((t)^2 - (0)^2) + Q'_{ij_\bullet}((2t)^2 - (t)^2) + Q'_{ij+}((3t)^2 - (2t)^2) + Q'_{ij_\circ}((4t)^2 - (3t)^2))\}/2 \quad (6)$$

and subscripts i, j = 1, 2, 6.
The coupling stiffness contribution from the angle plies is therefore:

$$B_{ij+} = -2t^2/2 \times Q'_{ij+} \quad (7)$$

$$B_{ij-} = -2t^2/2 \times Q'_{ij-} \quad (8)$$

and from the cross-plies:

$$B_{ij_\circ} = t^2/2 \times Q'_{ij_\circ} \quad (9)$$

$$B_{ij_\bullet} = 3t^2/2 \times Q'_{ij_\bullet} \quad (10)$$

These coupling stiffness terms may also be written in alternative form:

$$B_{ij+} = \chi_+ t^2/4 \times Q'_{ij+} \quad (11)$$

$$B_{ij-} = \chi_- t^2/4 \times Q'_{ij-} \quad (12)$$

$$B_{ij_\circ} = \chi_\circ t^2/4 \times Q'_{ij_\circ} \quad (13)$$

and

$$B_{ij_\bullet} = \chi_\bullet t^2/4 \times Q'_{ij_\bullet} \quad (14)$$

respectively, where $\chi_+ = \chi_- = -4$, $\chi_\circ = 2$ and $\chi_\bullet = 6$.
Similar non-dimensional parameters can be developed for the Extensional and Bending Stiffnesses. These non-dimensional parameters, together with the transformed reduced stiffness, Q'_{ij}, for each ply orientation and constant ply thickness, *t*, facilitate simple calculation of the elements of the extensional, coupling and bending stiffness matrices from:

$$\begin{aligned} A_{ij} &= \{n_+ Q'_{ij+} + n_- Q'_{ij-} + n_\circ Q'_{ij_\circ} + n_\bullet Q'_{ij_\bullet}\}t \\ B_{ij} &= \{\chi_+ Q'_{ij+} + \chi_- Q'_{ij-} + \chi_\circ Q'_{ij_\circ} + \chi_\bullet Q'_{ij_\bullet}\}t^2/4 \\ D_{ij} &= \{\zeta_+ Q'_{ij+} + \zeta_- Q'_{ij-} + \zeta_\circ Q'_{ij_\circ} + \zeta_\bullet Q'_{ij_\bullet}\}t^3/12 \end{aligned} \quad (15)$$

The elements of the thermal force resultant vector, arising from a temperature change, ΔT, follow from:

$$N_x^{\text{Thermal}} = \Delta T\{\Sigma n_\theta(Q'_{11\theta}\alpha'_{11\theta} + Q'_{12\theta}\alpha'_{22\theta} + Q'_{16\theta}\alpha'_{12\theta})\}t$$
$$N_y^{\text{Thermal}} = \Delta T\{\Sigma n_\theta(Q'_{21\theta}\alpha'_{11\theta} + Q'_{22\theta}\alpha'_{22\theta} + Q'_{26\theta}\alpha'_{12\theta})\}t$$
$$N_{xy}^{\text{Thermal}} = \Delta T\{\Sigma n_\theta(Q'_{61\theta}\alpha'_{11\theta} + Q'_{62\theta}\alpha'_{22\theta} + Q'_{66\theta}\alpha'_{12\theta})\}t$$
(16)

where the summations account for each of the ply orientations, θ = +, –, O and ●, and the elements of the thermal moment resultant vector, arising from a temperature change, ΔT, follow in a similar manner from:

$$M_x^{\text{Thermal}} = \Delta T\{\Sigma \chi_\theta(Q'_{11\theta}\alpha'_{11\theta} + Q'_{12\theta}\alpha'_{22\theta} + Q'_{16\theta}\alpha'_{12\theta})\}t^2/4$$
$$M_y^{\text{Thermal}} = \Delta T\{\Sigma \chi_\theta(Q'_{21\theta}\alpha'_{11\theta} + Q'_{22\theta}\alpha'_{22\theta} + Q'_{26\theta}\alpha'_{12\theta})\}t^2/4$$
$$M_{xy}^{\text{Thermal}} = \Delta T\{\Sigma \chi_\theta(Q'_{61\theta}\alpha'_{11\theta} + Q'_{62\theta}\alpha'_{22\theta} + Q'_{66\theta}\alpha'_{12\theta})\}t^2/4$$
(17)

The transformed reduced stiffnesses are defined by:

$$Q'_{11} = Q_{11}\cos^4\theta + 2(Q_{12} + 2Q_{66})\cos^2\theta\sin^2\theta + Q_{22}\sin^4\theta$$
$$Q'_{12} = Q'_{21} = (Q_{11} + Q_{22} - 4Q_{66})\cos^2\theta\sin^2\theta + Q_{12}(\cos^4\theta + \sin^4\theta)$$
$$Q'_{16} = Q'_{61} = \{(Q_{11} - Q_{12} - 2Q_{66})\cos^2\theta + (Q_{12} - Q_{22} + 2Q_{66})\sin^2\theta\}\cos\theta\sin\theta$$
$$Q'_{22} = Q_{11}\sin^4\theta + 2(Q_{12} + 2Q_{66})\cos^2\theta\sin^2\theta + Q_{22}\cos^4\theta$$
$$Q'_{26} = Q'_{62} = \{(Q_{11} - Q_{12} - 2Q_{66})\sin^2\theta + (Q_{12} - Q_{22} + 2Q_{66})\cos^2\theta\}\cos\theta\sin\theta$$
$$Q'_{66} = (Q_{11} + Q_{22} - 2Q_{12} - 2Q_{66})\cos^2\theta\sin^2\theta + Q_{66}(\cos^4\theta + \sin^4\theta)$$
(18)

and the transformed thermal expansion coefficients by:

$$\alpha'_{11} = \alpha_{11}\cos^2\theta + \alpha_{22}\sin^2\theta - \alpha_{12}\cos\theta\sin\theta$$
$$\alpha'_{22} = \alpha_{11}\sin^2\theta + \alpha_{22}\cos^2\theta + \alpha_{12}\cos\theta\sin\theta$$
$$\alpha'_{12} = 2\alpha_{11}\cos\theta\sin\theta - 2\alpha_{22}\cos\theta\sin\theta + \alpha_{12}(\cos^2\theta - \sin^2\theta)$$
(19)

noting that the thermal shearing coefficient, α_{12}, is zero for unidirectional plies, giving zero transformed thermal shearing coefficients, $\alpha'_{12_O} = \alpha'_{12_●} = 0$, when θ = O and ●, in Eqs (16) and (17).

3.2 Assessment of thermal response.

For non-standard fibre angles θ = 60°, -60°, 0° and 90° in place of symbols +, –, O and ● respectively, the transformed reduced stiffness, Q'_{ij} (N/mm^2), and thermal expansion coefficient, α'_{ij} (/°C), for typical IM7/8552 carbon-fibre/epoxy are given in Tables 2 and 3, respectively.

The **ABD** relation for the 8-ply laminate [+/O/–/O/–/●/+/O]$_T$, now becomes:

$$\begin{Bmatrix} N_x \\ N_y \\ N_{xy} \end{Bmatrix} = \begin{bmatrix} 82{,}154 & 20{,}048 & 0 \\ & 82{,}154 & 0 \\ \text{Sym.} & & 20{,}943 \end{bmatrix} \begin{Bmatrix} \varepsilon_x \\ \varepsilon_y \\ \gamma_{xy} \end{Bmatrix} + \begin{bmatrix} 1{,}059 & -1{,}059 & 0 \\ & 1{,}059 & 0 \\ \text{Sym.} & & -1{,}059 \end{bmatrix} \begin{Bmatrix} \kappa_x \\ \kappa_y \\ \kappa_{xy} \end{Bmatrix}$$

$$\begin{Bmatrix} M_x \\ M_y \\ M_{xy} \end{Bmatrix} = \begin{bmatrix} 1{,}059 & -1{,}059 & 0 \\ & 1{,}059 & 0 \\ \text{Sym.} & & -1{,}059 \end{bmatrix} \begin{Bmatrix} \varepsilon_x \\ \varepsilon_y \\ \gamma_{xy} \end{Bmatrix} + \begin{bmatrix} 9{,}787 & 2{,}087 & 744 \\ & 7{,}315 & 2{,}111 \\ \text{Sym.} & & 2{,}180 \end{bmatrix} \begin{Bmatrix} \kappa_x \\ \kappa_y \\ \kappa_{xy} \end{Bmatrix}$$

(20)

and for a temperature change of -180°C, typical of the cooling phase in a high temperature curing process, the vectors of force and moment resultants become:

$$\{N_x^{Thermal}, N_y^{Thermal}, N_{xy}^{Thermal}\} = \{-38.5, -38.5, 0\} \text{ N/mm}$$
$$\{M_x^{Thermal}, M_y^{Thermal}, M_{xy}^{Thermal}\} = \{0, 0, 0\} \text{ N.mm/mm}$$

(21)

Inspection of the extensional stiffness [**A**] matrix reveals that $A_{11} = A_{22}$, but calculation reveals that $A_{66} \neq (A_{11} - A_{12})/2 = 25{,}998$ N/mm^2, hence the laminate does not possess in-plane isotropic properties. Instead the laminate possesses square symmetry, defined elsewhere [12] as equal stiffness on principal axes, as would be the case in a cross-ply laminate or a fabric with balanced weave. Note that square symmetry also exists in the presence of shear-extension coupling (which arises for off-axis material alignment) where $A_{11} = A_{22}$ and $A_{26} = -A_{16}$. Square symmetry is also revealed in the coupling stiffness [**B**] matrix and the thermal load vector {**N**}, which equates to thermally isotropic behaviour [11]. The significance of square symmetry is revealed from inspection of the inverse of the **ABD** relation and the resulting in-plane strains, $\{\boldsymbol{\varepsilon}\} = [\mathbf{a}]\{\mathbf{N}\}$, and curvatures, $\{\boldsymbol{\kappa}\} = [\mathbf{b}]^T\{\mathbf{N}\}$.

The inverse relationships reveal that the matrix of in-plane compliances, {**a**}, remains square symmetric, but the matrix of coupling compliances, $\{\mathbf{b}\}^T$, does not:

$$\begin{bmatrix} b_{11} & -b_{11} & b_{61} \\ -b_{22} & b_{22} & b_{62} \\ b_{16} & -b_{16} & b_{66} \end{bmatrix}$$

(22)

Instead, $\{\mathbf{b}\}^T$ possesses a special form, relating the first two columns as follows: $b_{21} = -b_{11}$, $b_{12} = -b_{22}$ and, when present, $b_{16} = -b_{26}$.

Hence, this is an <u>*E-B-S-T*;*B-T*</u> coupled laminate, exhibiting equal thermal strains in the principal axis directions and no thermal shearing strains, hence from $\{\boldsymbol{\varepsilon}\} = [\mathbf{a}]\{\mathbf{N}\}$:

$$\{\varepsilon_x, \varepsilon_y, \gamma_{xy}\} = \{-376.5\mu, -376.5\mu, 0\} \tag{23}$$

but more significantly, no curvatures are developed as a result of the temperature change, which are revealed from $\{\boldsymbol{\kappa}\} = [\mathbf{b}]^{\mathbf{T}}\{\mathbf{N}\}$:

$$\{\kappa_x, \kappa_y, \kappa_{xy}\} = \{0, 0, 0\} \tag{24}$$

This laminate therefore exhibits HTCS behaviour. Hence, square symmetry in [**A**], [**B**] and {**N**}, with {**M**} = {**0**}, are shown to be the necessary conditions for hygro-thermally curvature-stable laminates.

3.3 Necessary conditions for HTCS laminates.

The necessary conditions for HTCS behaviour can be found in numerous articles [2,4,5,7,11], and are summarized here, in Table 4, in terms of the equivalent form of the extensional and coupling stiffness matrices, which vary with material axis alignment, β; noting that the form of the bending stiffness matrix has no influence on the HTCS behaviour. These square symmetric stiffness matrices are ply angle dependent and therefore the non-dimensional parameters are unrevealing in the search for HTCS laminates.

Lamination parameters, originally conceived by Tsai and Hahn [12], offer an alternative and, in fact, a more efficient set of non-dimensional expressions when ply angles are a design constraint. These ply angle dependent lamination parameters are readily derived from the non-dimensional parameters by the following expressions:

$$\begin{aligned}
\xi_1 = \xi_1^{A} &= \{n_+\cos(2\theta_+) + n_-\cos(2\theta_-) + n_\circ\cos(2\theta_\circ) + n_\bullet\cos(2\theta_\bullet)\}/n \\
\xi_2 = \xi_2^{A} &= \{n_+\cos(4\theta_+) + n_-\cos(4\theta_-) + n_\circ\cos(4\theta_\circ) + n_\bullet\cos(4\theta_\bullet)\}/n \\
\xi_3 = \xi_3^{A} &= \{n_+\sin(2\theta_+) + n_-\sin(2\theta_-) + n_\circ\sin(2\theta_\circ) + n_\bullet\sin(2\theta_\bullet)\}/n \\
\xi_4 = \xi_4^{A} &= \{n_+\sin(4\theta_+) + n_-\sin(4\theta_-) + n_\circ\sin(4\theta_\circ) + n_\bullet\sin(4\theta_\bullet)\}/n
\end{aligned} \tag{25}$$

$$\begin{aligned}
\xi_5 = \xi_1^{B} &= \{\chi_+\cos(2\theta_+) + \chi_-\cos(2\theta_-) + \chi_\circ\cos(2\theta_\circ) + \chi_\bullet\cos(2\theta_\bullet)\}/n^2 \\
\xi_6 = \xi_2^{B} &= \{\chi_+\cos(4\theta_+) + \chi_-\cos(4\theta_-) + \chi_\circ\cos(4\theta_\circ) + \chi_\bullet\cos(4\theta_\bullet)\}/n^2 \\
\xi_7 = \xi_3^{B} &= \{\chi_+\sin(2\theta_+) + \chi_-\sin(2\theta_-) + \chi_\circ\sin(2\theta_\circ) + \chi_\bullet\sin(2\theta_\bullet)\}/n^2 \\
\xi_8 = \xi_4^{B} &= \{\chi_+\sin(4\theta_+) + \chi_-\sin(4\theta_-) + \chi_\circ\sin(4\theta_\circ) + \chi_\bullet\sin(4\theta_\bullet)\}/n^2
\end{aligned} \tag{26}$$

$$\begin{aligned}
\xi_9 = \xi_1^{D} &= \{\zeta_+\cos(2\theta_+) + \zeta_-\cos(2\theta_-) + \zeta_\circ\cos(2\theta_\circ) + \zeta_\bullet\cos(2\theta_\bullet)\}/n^3 \\
\xi_{10} = \xi_2^{D} &= \{\zeta_+\cos(4\theta_+) + \zeta_-\cos(4\theta_-) + \zeta_\circ\cos(4\theta_\circ) + \zeta_\bullet\cos(4\theta_\bullet)\}/n^3 \\
\xi_{11} = \xi_3^{D} &= \{\zeta_+\sin(2\theta_+) + \zeta_-\sin(2\theta_-) + \zeta_\circ\sin(2\theta_\circ) + \zeta_\bullet\sin(2\theta_\bullet)\}/n^3 \\
\xi_{12} = \xi_4^{D} &= \{\zeta_+\sin(4\theta_+) + \zeta_-\sin(4\theta_-) + \zeta_\circ\sin(4\theta_\circ) + \zeta_\bullet\sin(4\theta_\bullet)\}/n^3
\end{aligned} \tag{27}$$

Elements of the thermal force and moment resultants are related to the non-dimensional parameters by Eq. (16) and Eq. (17), respectively, but may also be related to the lamination parameters [12], laminate invariants and thermal coefficients by:

$$N_x^{\text{Thermal}} = \Delta T\{U_1^{\text{Thermal}} + \xi_1 U_2^{\text{Thermal}}\} \times H/2$$
$$N_y^{\text{Thermal}} = \Delta T\{U_1^{\text{Thermal}} - \xi_1 U_2^{\text{Thermal}}\} \times H/2$$
$$N_{xy}^{\text{Thermal}} = \Delta T\{\xi_3 U_2^{\text{Thermal}}\} \times H/2 \qquad (28)$$

$$M_x^{\text{Thermal}} = \Delta T\{\xi_5 U_2^{\text{Thermal}}\} \times H^2/8$$
$$M_y^{\text{Thermal}} = \Delta T\{-\xi_5 U_2^{\text{Thermal}}\} \times H^2/8$$
$$M_{xy}^{\text{Thermal}} = \Delta T\{\xi_7 U_2^{\text{Thermal}}\} \times H^2/8 \qquad (29)$$

where inspection of Eq. (26) confirms that square symmetry in the thermal load vector $\{\mathbf{N}\}$, which equates to thermally isotropic behaviour, requires $\xi_1 = \xi_3 = 0$, see Table 4. Laminate invariants are calculated from the reduced stiffness terms, Q_{ij}:

$$U_1 = \{3Q_{11} + 3Q_{22} + 2Q_{12} + 4Q_{66}\}/8$$
$$U_2 = \{Q_{11} - Q_{22}\}/2$$
$$U_3 = \{Q_{11} + Q_{22} - 2Q_{12} - 4Q_{66}\}/8$$
$$U_4 = \{Q_{11} + Q_{22} + 6Q_{12} - 4Q_{66}\}/8$$
$$U_5 = \{Q_{11} + Q_{22} - 2Q_{12} + 4Q_{66}\}/8 \qquad (30)$$

and thermal coefficients:

$$U_1^{\text{Thermal}} = \alpha_{11}Q_{11} + (\alpha_{11} + \alpha_{22})Q_{12} + \alpha_{22}Q_{22}$$
$$U_2^{\text{Thermal}} = \alpha_{11}Q_{11} + (\alpha_{22} - \alpha_{11})Q_{12} + \alpha_{22}Q_{22} \qquad (31)$$

Finally, the reduced stiffness terms are calculated from the material properties:

$$Q_{11} = E_1/(1 - \nu_{12}\nu_{21})$$
$$Q_{12} = \nu_{12}E_2/(1 - \nu_{12}\nu_{21})$$
$$Q_{22} = E_2/(1 - \nu_{12}\nu_{21})$$
$$Q_{66} = G_{12} \qquad (32)$$

4. Results and Discussion.

The HTCS laminate solutions presented in this section, which contain non-standard ply orientations (+60, -60, 0 and 90°), have been algorithmically filtered from the definitive listings developed previously [1] for $\mathbf{A_S B_S D_F}$ or *B-E-T-S;B-T* coupled laminates and $\mathbf{A_S B_S D_S}$ or *B-E-T-S* coupled laminates using the necessary conditions for HTCS behaviour presented in Table 4. These are the parent laminate classes for HTCS behaviour and give rise to Bending-Twisting and/or Extension-Bending and Shearing-Twisting, respectively. Other classes of mechanically coupled laminate can be achieved through off-axis materials alignment of these parent classes, thus preserving the HTCS behaviour.

4.1 HTCS laminate solutions

Cross et al. [5] provide an important clue to discovering HTCS laminates with non-

standard ply orientations: repeating cross-ply sub-laminates considered an essential prerequisite by others [3,7] were absent in a small number of the HTCS configurations presented, but no further insight was provided. In fact these configurations contain a mixture of $\pi/3$ extensionally isotropic sub-laminates and cross-ply sub-laminates; the result of which is a transformation from uncoupled isotropic properties to mechanically coupled HTCS properties. This transformation can be understood from the well-known fact [9] that the addition of cross-plies to an otherwise uncoupled laminate renders the laminate coupled in Extension-Bending and Shearing-Twisting; one of the two parent classes for HTCS laminates.

The concept can be very clearly seen from one of the new laminate solutions discovered: $[+/-/\text{O}/-/\text{O}/+/\text{O}/+/-/\underline{\text{O}}/\underline{\bullet}/\underline{\bullet}/\underline{\text{O}}]_T$, where +, −, O and ● become +60, -60, 0 and 90° (or +30, -30, 90 and 0°), i.e., $[60/\text{-}60/0/\text{-}60/0/60/0/60/\text{-}60/\underline{0}/\underline{90}/\underline{90}/\underline{0}]_T$. Here, the first nine plies of this 13-ply stacking sequence represent a quasi-isotropic laminate: $[60/\text{-}60/0/\text{-}60/0/60/0/60/\text{-}60]_T$, with Bending-Twisting coupling, but the addition of the cross-ply sub-laminate $[\underline{0}/\underline{90}/\underline{90}/\underline{0}]_T$ to the outer surface, underlined for clarity, results in a hygro-thermally curvature stable $\mathbf{A}_S\mathbf{B}_S\mathbf{D}_S$ laminate; or *B-E-T-S* coupled.

By contrast, the single 8-ply $\mathbf{A}_S\mathbf{B}_S\mathbf{D}_F$: $[+/\text{O}/-/\text{O}/-/\underline{\bullet}/+/\underline{\text{O}}]_T$, i.e. $[60/0/\text{-}60/0/\text{-}60/\underline{90}/60/\underline{0}]_T$, or *B-E-T-S*;*B-T* coupled laminate, illustrates a clear example where the (underlined) cross-ply and $\pi/3$ extensionally isotropic sub-laminates are interlaced rather than added. Several 8-ply solutions were presented by Cross et al. [5], but all correspond to the sequence above; modified by either off-axis rotation, β, reversal of the stacking sequence or sign switching, i.e., 60° plies are exchanged with -60° plies and vice versa.

In addition to the discovery of two new 13-ply laminate solutions, described above, the second differing from the first by a switch in the positions of the four outer cross-plies, i.e., 0° plies are exchanged with 90° plies and vice versa, the number of solutions from the *B-E-T-S* coupled parent class increases to 19, 76, 89, etc., for 15-, 16-, 17-ply laminates, respectively, see Table 5. Examples for each ply number grouping, n, are given in Table 6, which are ordered by increasing n, then by the number of angle plies, $n_{\pm}$, then cross plies, n_{O} then $n_{\bullet}$, and finally by B_{16}, then D_{16}, based on an off-axis material alignment, $\beta = \pi/8$; chosen because Extension-Twisting coupling is the simplest response to validate experimentally.

Similarly for the *B-E-T-S*;*B-T* coupled parent class, the number of solutions increases from the single 8-ply laminate solution, to 8, 14, 40, 135, etc. for 10-, 11-, 12-, 13-ply laminates, respectively, see Table 5. Example stacking sequences for each ply number grouping are given in Table 7, using the same criteria applied to Table 6.

The number of solutions for non-standard ply orientations may be compared with laminate designs for standard ply orientations [2], for which there are 6, 524, and 35,610 with 12, 16 and 20 plies from the *B-E-T-S* couple parent class and 410, 40,808 and 4,515,473 with 12, 16 and 20 plies, respectively, for the *B-E-T-S*;*B-T* coupled parent class.

Off-axis orientation of these two parent classes, represented by the centre illustrations in Figs 1 and 2, respectively, give rise to all nine classes illustrated in Figs 1 – 3 for standard ply orientations. By contrast, only four of the coupled laminate classes illustrated in Figs 1 – 3 are possible with non-standard ply orientations. An off-axis alignment $\beta = \pi/8$ (or 22.5°) transforms both parent classes into *E-S*;*E-T-S-B*;*B-T* coupled ($\mathbf{A}_F\mathbf{B}_t\mathbf{D}_F$) laminates, and for general off-axis orientation, β, transforms both

parent classes into *E-S*; *E-B*-*S-B*-*E-T*-*S-T*;*B-T* coupled ($\mathbf{A}_F\mathbf{B}_F\mathbf{D}_F$) laminates; representing laminate classes illustrated in Fig. 3.
This limitation is explained by a comparison of the form of the stacking sequences with standard and non-standard ply orientations. For HTCS laminate designs with standard ply orientations, cross-plies and angle-plies occur in balanced pairs, hence an off-axis rotation of $\pi/8$ (or 22.5°) produces a balanced double-angle-ply laminate when the number of cross-ply and angle-ply pairs are equal, leading to uncoupled bending and/or extensional stiffness properties. By contrast, only angle-plies are balanced in laminates with non-standard ply orientations, hence coupled bending and/or extensional behaviour can only be avoided for off-axis alignments, $\beta = m\pi/2$ (m = 0, 1, 2 and 3).
The strength of the mechanical coupling achievable with non-standard ply orientations is, in general, of a lower magnitude than that achievable with standard ply orientations. This comparison is demonstrated by polar plots of the lamination parameters, where the highest coupling magnitude achievable from the non-standard 16-ply solutions, illustrated in Fig. 4, may be compared with that of a laminate developed previously [13] with standard ply orientations ±45, 0 and 90°, illustrated in Fig. 5; a laminate with isotropic extensional stiffness and isotropic bending stiffness, for which the corresponding lamination parameters, ξ_1 - ξ_4 and ξ_9 - ξ_{12}, are zero and are therefore not shown.
Comparison of the lamination parameters in Figs 4(b) and 5, for ξ_5 - ξ_8, reveals that whilst the coupling magnitude can be maximised for standard ply orientations, only approximately half this magnitude is attainable for non-standard orientations; which is in fact a common feature across all the ply number groupings investigated.

4.2 Tapered HTCS laminates.

The requirement for tapered thickness in mechanically coupled laminate designs adds a significant complication. Practical designs must offer the possibility for individual or grouped ply terminations, in order to reduce the laminate thickness, but without affecting the nature of the mechanical coupling behaviour or the immunity to thermal distortion during manufacture; a subject not previously been considered in the literature. In fact many HTCS laminate designs have been obtained by employing mathematical optimization strategies to maximize the mechanical coupling response and, as a result, these often contain layers with highly irregular ply orientations; in such cases, ply terminations inevitably destroy both the form of the mechanical coupling response and thermal shape stability.
The tapered solutions reported here were developed in a two-stage process. Firstly, each ply number grouping, n, was screened against higher ply number groupings, $n + 2$ and $n + 4$. Odd ply number groupings were also screened to confirm the hypothesis that plies must be terminated in orthogonal pairs to maintain the necessary square symmetry. Results from the first stage were then screened for compatibility in a second stage: this time over a range of ply number groupings.
The example stacking sequences listed in Tables 6 and 7 suggest that there may be greater scope for tapering non-standard ply orientation designs, compared with standard ply orientation designs, given that HTCS solutions exist for all consecutive ply number groupings above 10 plies, rather than only as multiples of 4 plies; within the range of up to 21 ply laminates. However, careful comparison of the form of the stacking sequences for odd and even ply laminates, see Tables 6 and 7, reveals that a change in the ply

number grouping from n to $n + 1$, results in a change in the number of angle plies from $n_{\pm}$ to $n_{\pm} + 2$, which therefore precludes single ply terminations. Furthermore, 2-ply terminations were found to give limited scope for tapered laminates, given that solutions were found only in the higher ply number groupings and across a very limited range, e.g. whilst there are many 20-18-ply tapered laminates, none provide a compatible match with the single 18-16-ply tapered laminate identified, i.e.:

$[+/\bullet/\bullet/O/O/-/O/O/O/\underline{\bullet}/+/-/\underline{O}/-/-/O/+/+]_T$

$[+/\bullet/\bullet/O/O/-/O/O/O/+/-/-/-/O/+/+]_T$

(33)

where terminated plies are underlined for clarity.

By contrast, the introduction of 4-ply terminations gives substantial scope for tailoring. For example, introducing 4-ply terminations into 16-ply laminates, for which there are 4,213 HTCS stacking sequences, produces 8,533 compatible designs, which match the 40 HTCS stacking sequences with 12 plies; some stacking sequences produce multiple compatible designs by terminating different ply combinations. Introducing further 4-ply terminations produces 46 compatible designs matching the single HTCS stacking sequence with 8 plies.

Despite the substantial number of 16-12-8-ply tapered HTCS laminates identified, all are however restricted entirely to cross-ply sub-sequence terminations, e.g.:

$[+/O/\underline{\bullet}/-/O/-/\underline{O}/\bullet/+/\underline{O}/O/O/\underline{\bullet}/\bullet/\bullet/O]_T$

$[+/O/-/O/-/\bullet/+/\underline{O}/\underline{O}/\underline{\bullet}/\underline{\bullet}/O]_T$

$[+/O/-/O/-/\bullet/+/O]_T$

(34)

$[+/\bullet/O/-/O/O/\underline{\bullet}/\underline{O}/O/-/\bullet/\bullet/+/\underline{O}/\underline{\bullet}/O]_T$

$[+/\underline{\bullet}/O/-/\underline{O}/O/\underline{O}/-/\bullet/\underline{\bullet}/+/O]_T$

$[+/O/-/O/-/\bullet/+/O]_T$

(35)

This restriction also follows for tapered sequences with odd ply number groupings, e.g. 15-11-ply tapered HTCS laminate:

$[+/O/-/+/\underline{\bullet}/O/\underline{O}/-/-/O/\underline{O}/\bullet/\underline{\bullet}/O/+]_T$

$[+/O/-/+/O/-/-/O/\bullet/O/+]_T$

(36)

By contrast, the use of standard ply orientations, where symbols +, −, O and ● now represent ply orientations: +45, -45, 0, 90°, respectively, the following 16-12-8-ply tapered HTCS laminate:

$[+/-/\bigcirc/+/\bullet/-/-/\bullet/\underline{+}/\bigcirc/\underline{-}/+/\underline{\bigcirc}/\underline{\bullet}/\bullet/\bigcirc]_T$

$[+/-/\bigcirc/\underline{+}/\bullet/\underline{-}/-/\underline{\bullet}/\underline{\bigcirc}/+/\bullet/\bigcirc]_T$

$[+/-/\bigcirc/\bullet/-/+/\bullet/\bigcirc]_T$

has been discovered, which demonstrates that both angle- and cross-ply terminations are possible. In fact many solutions exist, but this example has been chosen because it has special significance due to identical normalised [11, 12] square symmetric stiffness properties, i.e., [**A**]* as well as [**B**]* in each of the three stacking sequences; which is of particular interest in the investigation of unique laminated composite material properties. More will be said in a subsequent article concerning the tapering of HTCS laminates with standard ply orientations.

Experimental results [10] have demonstrated the validity of the HTCS stacking sequences for standard ply orientations, but the results of the present article, with non-standard ply orientations, including the influence of taper, have yet to be validated.

5. Conclusions.

Design solutions for Hygro-Thermally Curvature-Stable (HTCS) laminates with non-standard ply angle orientations (+60, −60, 0 and 90°) have been discovered in all ply number groupings with 10 plies and above; thus extending the scope for laminate design beyond that achievable with standard ply angle orientations (+45, −45, 0 and 90°), where solutions are restricted to 8-, 12-, 16- and 20-ply laminates, etc.
Laminates with non-standard ply angle orientations contain combinations of $\pi/3$ extensionally isotropic and cross-ply sub-laminates; the result being a transformation from uncoupled isotropic properties to coupled HTCS solutions. In the vast majority of cases, these sub-laminates were interlaced rather than added, leading to stacking sequence configurations with no discernable patterns, such as sub-symmetries or repeating sub-laminates, suggested in the literature.
The number of distinct classes of mechanical coupling behaviour in HTCS laminates with non-standard ply orientations is reduced to only four of the nine distinct classes found in their standard ply orientation counterparts.
Tapered laminates are generally restricted to a minimum of 4-ply terminations in order to preserve both mechanical coupling and HTCS behaviour; 2-ply terminations were possible only in laminates with 18 plies and above.
Tapered laminates with non-standard ply orientations are further restricted to cross-ply terminations only. However, this is not the case for tapered laminates with standard ply orientations, for which combinations of both cross-ply and angle-ply terminations have been identified.

References.

[1] C. B. York "Unified approach to the characterization of coupled composite laminates: Benchmark configurations and special Cases". *Journal of Aerospace Engineering, ASCE,* Vol. 23, No. 4, pp. 219-42, 2010.

[2] C. B. York "Unified approach to the characterization of coupled composite laminates: Hygro-thermally curvature-stable configurations". *International Journal of Structural Integrity*, Vol. 2, No. 4, pp. 406-36, 2011.

[3] S. J. Winckler "Hygrothermally curvature stable laminates with tension-torsion coupling". *Journal of the American Helicopter Society*, Vol. 31, pp. 56-58, 1985

[4] H. P. Chen "Study of hygrothermal isotropic layup and hygrothermal curvature-stable coupling composite laminates". *Proc. 44th AIAA/ASME/ ASCE/AHS/ASC Structures, Structural Dynamics, and Materials Conf.*, AIAA-2003-1506, 2003.

[5] R. J. Cross, R. A. Haynes and E. A. Armanios "Families of hygrothermally stable asymmetric laminated composites", *Journal of Composite Materials*, Vol. 42, pp. 697-716, 2008.

[6] R. Haynes and E. Armanios "Hygrothermally stable extension-twist coupled laminates with bending-twist couplined Laminates". *Proc. American Helicopter Society 67th Annual Forum*, Virginia, USA, 2011.

[7] P. M. Weaver “Anisotropic Laminates that Resist Warping during Manufacture”. *Proc. 15th International Conference on Composite Materials*, Durban, South Africa, 2005.
[8] S. W. Tsai “*Composite Design*”. Third Edition, Think Composites, 1987.
[9] ESDU (1994). Stiffnesses of laminated plates, Engineering Sciences Data Unit, Item No. 94003.
[10] J. Rousseau, G. Verchery and C. B. York “Experimental validation of laminated composites with thermal and/or mechanical coupling response: a search for hygro-thermally curvature-stable designs”. *Proc. 11th Deformation and Fracture of Composites and 5th Structural Integrity and Multi-scale Modelling Conference*, Cambridge, England, 2011.
[11] G. Verchery “Design rules for laminate stiffness”. *Mechanics of Composite Materials*, Vol. 47, pp. 47-58, 2011
[12] S. W. Tsai and H. T. Hahn “*Introduction to Composite Materials*”. Technomic Publishing Co. Inc., Lancaster, 1980.
[13] C. B. York “Coupled Quasi-Homogeneous Orthotropic Laminates”. *Mechanics of Composite Materials*, Vol. 47, No. 4, 2011.

Figures

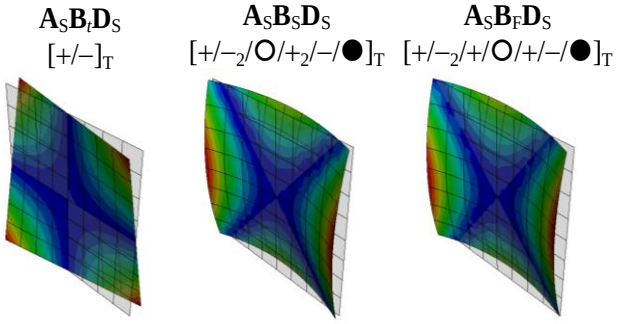

Figure 1 – Coupling responses, due to cooling without mechanical or geometrical constraint, for the: ($\mathbf{A_S B_t D_S}$) *B-S*-*T-E* laminate with Bending-Shearing and Twisting-Extension coupling; ($\mathbf{A_S B_S D_S}$) *B-E*-*T-S* laminate with Bending-Extension and Twisting-Shearing coupling and; ($\mathbf{A_S B_F D_S}$) *B-E*-*B-S*-*T-E*-*T-S* laminate with Bending-Extension, Bending-Shearing, Twisting-Extension, Twisting-Shearing coupling.

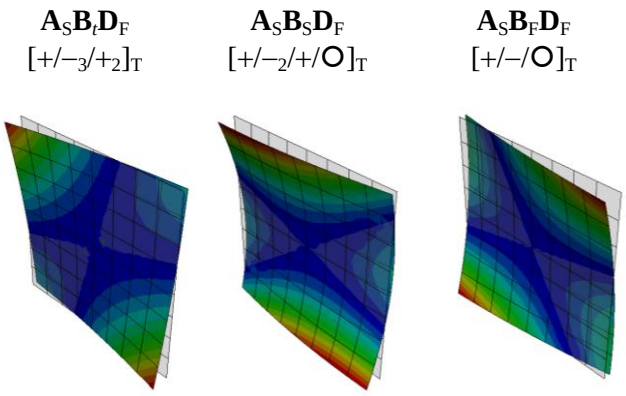

Figure 2 – Coupling responses, due to cooling without mechanical or geometrical constraint, for laminates with: ($\mathbf{A_S B_t D_F}$) *B-S*-*T-E*;*B-T* or Bending-Shearing, Twisting-Extension and Bending-Twisting coupling; ($\mathbf{A_S B_S D_F}$) *B-E*-*T-S*;*B-T* or Bending-Extension, Twisting-Shearing and Bending-Twisting coupling and; ($\mathbf{A_S B_F D_F}$) *B-E*-*B-S*-*T-E*-*T-S*;*B-T* or Bending-Extension, Bending-Shearing, Twisting-Extension, Twisting-Shearing and Bending-Twisting coupling.

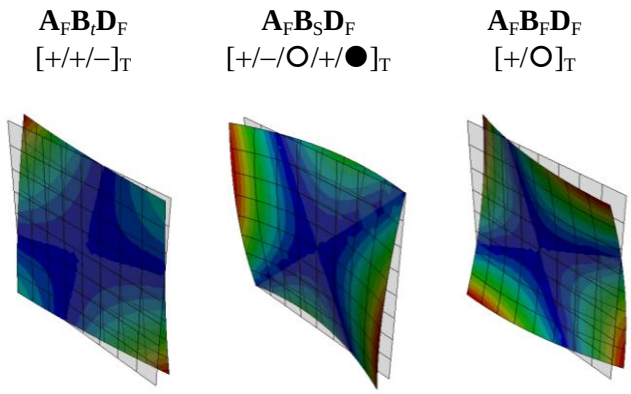

Figure 3 – Coupling responses, due to cooling without mechanical or geometrical constraint, for laminates with: ($\mathbf{A}_F\mathbf{B}_t\mathbf{D}_F$) *E-S*;*B-S*-*T-E*;*B-T* or Extension-Shearing, Bending-Shearing, Twisting-Extension and Bending-Twisting coupling; ($\mathbf{A}_F\mathbf{B}_S\mathbf{D}_F$) *E-S*;*B-E*-*T-S*;*B-T* or Extension-Shearing, Bending-Extension and Twisting-Shearing and Bending-Twisting coupling and; ($\mathbf{A}_F\mathbf{B}_F\mathbf{D}_F$) *E-S*;*B-E*-*B-S*-*T-E*-*T-S*;*B-T* or fully coupled laminate.

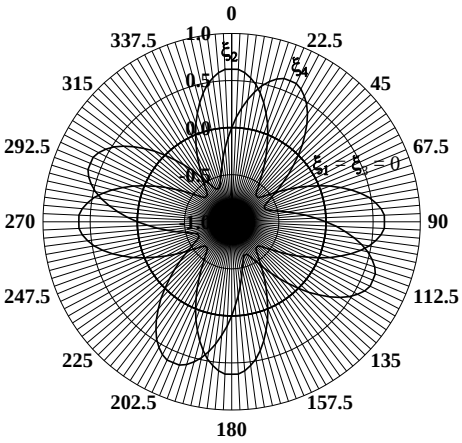

(a)

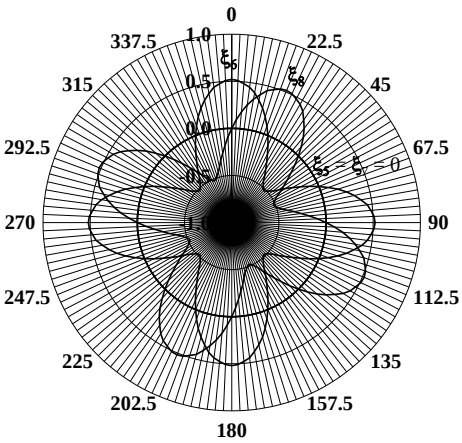

(b)

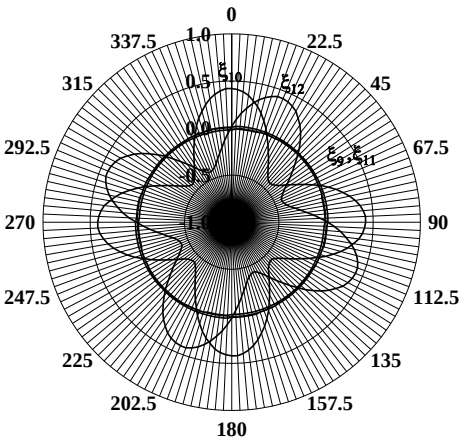

(c)

Figure 4 – Polar plots of lamination parameters (top) ξ_1 - ξ_4; (middle) ξ_5 - ξ_8; (bottom) ξ_9 - ξ_{12} corresponding to off-axis material alignment, β, for the 16-ply hygro-thermally curvature-stable laminate stacking sequence $[+/-/\text{O}/-/+/\text{O}_3/\bullet/\text{O}/\bullet_4/\text{O}_2]_T$, with non-standard ply orientations ±60, 0 and 90° in place of symbols +, –, O and ●, respectively.

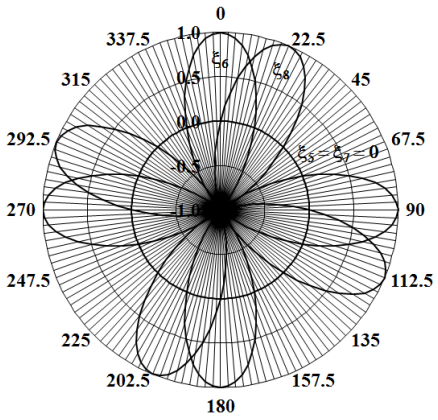

Figure 5 – Polar plot of lamination parameters ξ_5 - ξ_8, corresponding to off-axis material alignment, β, for the 16-ply HTCS laminate with Isotropic extensional and bending stiffness: $[+/-_2/+/-/+_2/-/O/\bullet_2/O/\bullet/O_2/\bullet]_T$, after Ref. [13], with standard ply orientations ±45, 0 and 90° in place of symbols +, –, O and ●, respectively.

Tables

Table 1 – Descriptions of coupling behaviour with subscript notation and associated form of stacking sequence for: (a) extensional stiffness matrix, **A**; (b) coupling stiffness matrix, **B**, and; (c) bending stiffness matrix, **D**. Subscript notation, relating to the form of the stiffness matrix, is described in the table footnotes.

(a)

Subscript notation	Response-based labelling	Matrix form
$\mathbf{A}_S$	Simple laminate	$\begin{bmatrix} A_{11} & A_{12} & 0 \\ A_{21} & A_{22} & 0 \\ 0 & 0 & A_{66} \end{bmatrix}$
$\mathbf{A}_F$	Shear-Extension; *S-E*	$\begin{bmatrix} A_{11} & A_{12} & A_{16} \\ A_{21} & A_{22} & A_{26} \\ A_{61} & A_{62} & A_{66} \end{bmatrix}$

(b)

Subscript notation	Response-based labelling	Matrix form
$\mathbf{B}_t$	Extension-Twisting and Shearing-Bending; *E-T-S-B*	$\begin{bmatrix} 0 & 0 & B_{16} \\ 0 & 0 & B_{26} \\ B_{61} & B_{62} & 0 \end{bmatrix}$
$\mathbf{B}_S$	Extension-Bending and Shearing-Twisting; *E-B-S-T*	$\begin{bmatrix} B_{11} & B_{12} & 0 \\ B_{21} & B_{22} & 0 \\ 0 & 0 & B_{66} \end{bmatrix}$
$\mathbf{B}_F$	Extension-Bending, Shearing-Bending, Extension-Twisting, and Shearing-Twisting; *E-B-S-B-E-T-S-T*	$\begin{bmatrix} B_{11} & B_{12} & B_{16} \\ B_{21} & B_{22} & B_{26} \\ B_{61} & B_{62} & B_{66} \end{bmatrix}$

(c)

Subscript notation	Response-based labelling	Matrix form
$\mathbf{D}_S$	Simple laminate	$\begin{bmatrix} D_{11} & D_{12} & 0 \\ D_{21} & D_{22} & 0 \\ 0 & 0 & D_{66} \end{bmatrix}$
$\mathbf{D}_F$	Twisting-Bending; *T-B*	$\begin{bmatrix} D_{11} & D_{12} & D_{16} \\ D_{21} & D_{22} & D_{26} \\ D_{61} & D_{62} & D_{66} \end{bmatrix}$

Summary of Matrix sub-scripts

0	=	All elements (of stiffness matrix) zero.
F	=	All elements Finite.
I	=	Fully Isotropic form.
t	=	Off-diagonal elements (B_{16}, $B_{26} \neq 0$) of **B** matrix non-zero, all other elements zero.
S	=	Specially orthotropic (uncoupled) or Simple form; $B_{16} = B_{26} = 0$ when applied to **B** matrix.

Table 2 – Transformed reduced stiffnesses (N/mm^2).

θ	Q'_{11}	Q'_{12}	Q'_{16}	Q'_{22}	Q'_{26}	Q'_{66}
-60	22,149	31,508	-17,059	97,731	-48,396	32,309
60	22,149	31,508	17,059	97,731	48,396	32,309
0	162,660	4,369	0	11,497	0	5,170
90	11,497	4,369	0	162,660	0	5,170

Table 3 – Transformed thermal coefficients (/°C).

θ	α'_{11}	α'_{22}	α'_{12}
-60	18.2μ	6.06μ	21.1μ
60	18.2μ	6.06μ	-21.1μ
0	-0.0181μ	24.3μ	0μ
90	24.3μ	-0.0181μ	0μ

Table 4 – Conditions for hygro-thermally curvature-stable behaviour in coupled laminates with non-standard ply angle orientations +60, −60, 0 and 90°.

Lamination parameters and stiffness relationships with respect to material axis alignment, β.		
$\beta = m\pi/2$	$\beta = \pi/8 + m\pi/2$	$\beta \neq m\pi/2,\ \pi/8 + m\pi/2$
	(m = 0, 1, 2, 3)	
(A_S)	(A_F)	(A_F)
$\begin{bmatrix} A_{11} & A_{12} & 0 \\ A_{21} & A_{11} & 0 \\ 0 & 0 & A_{66} \end{bmatrix}$	$\begin{bmatrix} A_{11} & A_{12} & A_{16} \\ A_{12} & A_{11} & -A_{16} \\ A_{16} & -A_{16} & A_{66} \end{bmatrix}$	$\begin{bmatrix} A_{11} & A_{12} & A_{16} \\ A_{12} & A_{11} & -A_{16} \\ A_{16} & -A_{16} & A_{66} \end{bmatrix}$
$\xi_1 = \xi_3 = \xi_4 = 0$	$\xi_1 = \xi_2 = \xi_3 = 0$	$\xi_1 = \xi_3 = 0$
(B_S)	(B_t)	(B_F)
$\begin{bmatrix} B_{11} & -B_{11} & 0 \\ -B_{11} & B_{11} & 0 \\ 0 & 0 & -B_{11} \end{bmatrix}$	$\begin{bmatrix} 0 & 0 & B_{16} \\ 0 & 0 & -B_{16} \\ B_{16} & -B_{16} & 0 \end{bmatrix}$	$\begin{bmatrix} B_{11} & -B_{11} & B_{16} \\ -B_{11} & B_{11} & -B_{16} \\ B_{16} & -B_{16} & -B_{11} \end{bmatrix}$
$\xi_5 = \xi_7 = \xi_8 = 0$	$\xi_5 = \xi_6 = \xi_7 = 0$	$\xi_5 = \xi_7 = 0$

Table 5 – Number of coupled HTCS laminate stacking sequence solutions for non-standard ply angle orientations +60, −60, 0 and 90°, corresponding to the two parent classes.

Plies (n)	8	9	10	11	12	13	14	15	16	17	18	19	20	21
B-E-T-S	-	-	-	-	-	2	-	19	76	89	177	899	4,165	8,726
B-E-T-S;B-T	1	-	8	14	40	135	494	1,188	4,213	11,144	43,986	120,982	295,906	1,215,077

Table 6 – Abridged HTCS laminate stacking sequence listings with non-dimensional parameters derived from the $\mathbf{A}_S\mathbf{B}_S\mathbf{D}_S$ laminate class. Note that $n_- = (n_\pm - n_+)$ and $\zeta_- = (\zeta_\pm - \zeta_+)$ in Eq. (15). The first column contains the ply number grouping, n, followed by a ranking in the second column; corresponding to increasing B_{16}, and then D_{16}, for the off-axis aligned $\mathbf{A}_S\mathbf{B}_t\mathbf{D}_F$ laminate class.

n	$A_SB_SD_S$:	Sequence	$n_\pm$	$n_\circ$	$n_\bullet$	χ_-	χ_+	$\chi_\circ$	$\chi_\bullet$	ζ	$\zeta_\pm$	ζ_0	$\zeta_\bullet$	n_+	ζ_+
13	*1*	+ − ○ − ○ + ○ + − ● ○ ○ ●	6	5	2	-24	-24	12	36	2197	918	737	542	3	459
13	*2*	+ − ○ − ○ + ○ + − ○ ● ● ○	6	5	2	-24	-24	12	36	2197	918	785	494	3	459
15	*3*	+ − ● ○ ○ ○ − ○ ● + + ○ − ○ ●	6	6	3	-8	-8	4	12	3375	1494	978	903	3	747
:	:														
15	*21*	+ − − ○ + + − ○ ○ ○ ○ ● ● ●	6	6	3	-48	-48	24	72	3375	1494	558	1323	3	747
16	*22*	+ ● − ○ ○ − ○ ○ ● + ○ + − ○ + −	8	6	2	16	16	-8	-24	4096	2720	864	512	4	1360
:	:														
16	*97*	+ ○ − ○ − − + + ○ + ○ − ○ ● ● ○	8	6	2	-32	-32	16	48	4096	1472	1752	872	4	736
17	*98*	+ − ● ○ − ○ ○ + + ○ − ○ ○ + − − +	10	6	1	16	16	-8	-24	4913	3706	774	433	5	1853
:	:														
17	*129*	+ ○ ○ − − + − ○ − + + ○ + ○ ● − ○	10	6	1	-16	-16	8	24	4913	2266	2214	433	5	1133
17	*130*	+ ● ○ − − ○ ● ○ ○ + ○ ○ ● + ○ − ●	6	7	4	-8	-8	4	12	4913	2166	1147	1600	3	1083
:	:														
17	*186*	+ − ○ − ○ + ○ + − ○ ○ ● ● ● ● ○ ○	6	7	4	-48	-48	24	72	4913	1782	2095	1036	3	891
18	*187*	+ ● − ○ ○ ● − ○ ○ ○ + ○ ● + − ○ + −	8	7	3	20	20	-10	-30	5832	3632	1228	972	4	1816
:	:														
18	*363*	+ − ○ + − − ○ ○ ○ + ○ + ● − ● ○ ● ○	8	7	3	-44	-44	22	66	5832	2624	2020	1188	4	1312
19	*364*	+ ● ● − ○ ○ ○ − ○ ○ − + ○ + ○ + + − −	10	7	2	40	40	-20	-60	6859	4474	1027	1358	5	2237
:	:														

Table 7 – Abridged HTCS laminate stacking sequence listings with non-dimensional parameters derived from the $\mathbf{A}_S\mathbf{B}_S\mathbf{D}_F$ laminate class. Note that $n_- = (n_\pm - n_+)$ and $\zeta_- = (\zeta_\pm - \zeta_+)$ in Eq. (15). The first column contains the ply number grouping, n, followed by a ranking in the second column; corresponding to increasing B_{16}, and then D_{16}, for the off-axis aligned $\mathbf{A}_S\mathbf{B}_t\mathbf{D}_F$ laminate class.

n	$A_SB_SD_F$:	Sequence	$n_\pm$	$n_\circ$	$n_\bullet$	χ_-	χ_+	$\chi_\circ$	$\chi_\bullet$	ζ	$\zeta_\pm$	ζ_0	$\zeta_\bullet$	n_+	ζ_+
8	*1*	+ − ○ ● − + ● ○	4	3	1	-4	-4	2	6	512	256	228	28	2	32
10	*2*	+ − ○ ● ○ ○ − + ○ ●	4	4	2	-8	-8	4	12	1000	496	232	272	2	176
:	:														
10	*9*	+ ○ − − ○ + ○ ● ● ○	4	4	2	-16	-16	8	24	1000	352	424	224	2	104
11	*10*	+ − ● ○ ○ ○ − ○ + + −	6	4	1	8	8	-4	-12	1331	1110	112	109	3	507
:	:														
11	*23*	+ ○ − ○ + − − ○ ● + ○	6	4	1	-8	-8	4	12	1331	630	592	109	3	123
12	*24*	+ − ● ○ ○ ● ○ ○ ○ − + ●	4	5	3	-4	-4	2	6	1728	1000	212	516	2	392
:	:														
12	*63*	+ − ○ − + ○ ○ ○ ● ● ● ○	4	5	3	-28	-28	14	42	1728	712	548	468	2	320
13	*64*	+ ● − ○ ○ ● ○ ○ ○ − + − +	6	5	2	16	16	-8	-24	2197	1662	221	314	3	603
:	:														
13	*198*	+ ○ − ○ − + − + ○ ○ ● ● ○	6	5	2	-24	-24	12	36	2197	702	1001	494	3	243
14	*199*	+ − ● − ○ ○ ○ ○ + ○ + + − −	8	5	1	12	12	-6	-18	2744	2312	188	244	4	1384
:	:														
14	*520*	+ ○ ○ − + − ○ − − + + ● ○ ○	8	5	1	-12	-12	6	18	2744	1016	1484	244	4	208
14	*521*	+ ● − ● ○ ○ ○ ○ ○ − ○ + ● ●	4	6	4	-8	-8	4	12	2744	1072	288	1384	2	320
:	:														
14	*692*	+ − − + ○ ○ ○ ○ ● ○ ● ● ● ○	4	6	4	-40	-40	20	60	2744	1264	696	784	2	608
15	*693*	+ ● ● ○ − ○ ○ ○ ○ ○ ● ○ − − + +	6	6	3	24	24	-12	-36	3375	2214	378	783	3	603
:	:														